Hindawi
Advances in Materials Science and Engineering
Volume 2019, Article ID 8625371, 9 pages
https://doi.org/10.1155/2019/8625371

Research Article

Effect of Variable Thermal Conductivity on the Generalized Thermoelasticity Problems in a Fiber-Reinforced Anisotropic Half-Space

Chun-Bao Xiong, Li-Na Yu, and Yan-Bo Niu

School of Civil Engineering, Tianjin University, Tianjin 300072, China

Correspondence should be addressed to Li-Na Yu; yulina@tju.edu.cn

Received 23 April 2019; Accepted 28 July 2019; Published 3 September 2019

Academic Editor: Paweł Kłosowski

Fiber-reinforced materials have widespread applications, which prompt the study of the effect of fiber reinforcement. Research studies have indicated that thermal conductivity cannot be considered as a constant, which is closely related to temperature change. Based on those studies, we investigate the fiber-reinforced generalized thermoelasticity problem under thermal stress, with the consideration of the effect of temperature-dependent variable thermal conductivity. The problem is assessed according to the L-S theory. A fiber-reinforced anisotropic half-space is selected as the research model, and a region of its surface is subjected to a transient thermal shock. The time-domain finite element method is applied to analyze the nonlinear problem and derives the governing equations. The nondimensional displacement, stress, and temperature of the material are obtained and illustrated graphically. The numerical results reveal that the variable conductivity significantly influences the distribution of the field quantities under the fiber-reinforced effect. And also, the boundary point of thermal shock is the most affected. The obtained results in this paper can be applied to design the fiber-reinforced anisotropic composites under thermal load to satisfy some particular engineering requirements.

1. Introduction

Fiber reinforcement is an inherent property of materials that is considered an effect rather than a form of inclusion in it [1]. In an elastic state, the components of fiber-reinforced composites act as a single anisotropic unit without relative displacement [2–6]. Fiber-reinforced material produces higher specific strength and a larger specific modulus in the direction of fiber reinforcement. The material performance of fiber-reinforced composites is designable, and its corrosion resistance and durability are good. Those outstanding features inherent in fiber-reinforced composites have led to their widespread applications in aerospace, building engineering, automotive industries, and so on [7, 8]. Therefore, the fiber-reinforced effect of materials should be considered when studying mechanical behavior.

The assumption of infinite propagation speed of the thermal signal in classical thermoelasticity theory is inconsistent with the real phenomenon. Several generalized thermoelasticity theories have been developed to eliminate this paradox [9–12], such as L-S theory. It firstly used the Maxwell–Cattaneo law of heat conduction instead of the conventional Fourier's law and presented the generalized thermoelastic theory with one relaxation time, which has been proved to be well investigated and well established. For fiber-reinforced generalized thermoelasticity problems, Othman and Said [4] investigated the thermal shock of 2D fiber-reinforced materials and found that the temperature, displacement, and stress components change drastically at the front of the heat wave. Othman and Lotfy [13] compared coupling theory, G-L theory, and L-S theory to prove that the fiber reinforcement and the magnetic field significantly influenced the physical quantities, such as stress and strain. And also, the results from the three theories are in accordance with each other. Abouelregal and Zenkour [14] analyzed the effects of the fractional parameter, reinforcement, and rotation on the variations of different field quantities inside the elastic medium and found that fiber reinforcement plays an important role in the distributions of the field quantities. Abbas [15] investigated the generalized thermoelastic interaction of an infinite fiber-reinforced anisotropic plate containing a circular hole and found that field quantities are significantly varied in the presence and absence of reinforcement.

Thermal conductivity is an important parameter of a material which is typically considered constant. However, several experimental and theoretical studies have indicated that thermal conductivity is closely related to temperature change [16–22]. Xiong and Guo [23] validated the effects of variable temperature-dependent properties on field quantities based on a one-dimensional generalized magneto-thermoelastic problem. Wang et al. [24] studied generalized thermoelasticity with variable thermal material properties and found that variable thermal material properties significantly affect the thermoelastic behaviors, particularly the magnitude of thermoelastic response. Ezzat and El-Bary [25] examined the effects of variable thermal conductivity in a problem of a thermo-viscoelastic infinitely long hollow cylinder and discovered that all functions for the generalized theory with a variable thermal conductivity distinctly differ from those obtained for the generalized theory with a constant thermal conductivity. Abo-Dahab and Abbas [26] evaluated the thermal shock problem of generalized magneto-thermoelasticity and concluded that as the variable thermal conductivity increases, the temperature increases, whereas the radial and hoop stresses decrease. These studies demonstrated that variable thermal conductivity significantly influences the material properties and the distribution of field quantities [27]. Instantaneous changes of temperature can markedly change the thermal conductivity of a material. Therefore, the influence of temperature-dependent variable thermal conductivity must be considered in solving fiber-reinforced generalized thermoelasticity problems suffered from thermal stress.

Normal mode analysis is applicable only for solving the steady state problem, whereas integral transformation and time-domain finite element method are suitable for solving dynamic problems. Integral transforms, such as Fourier and Laplace transforms, have been widely used for processing the related generalized thermoelastic problems [28–30]. In considering the effect of temperature-dependent variable conductivity in the fiber-reinforced generalized thermoelasticity problem, the governing equation has a nonlinear form. Given that the governing equations contain higher-order terms and nonlinear coupling terms, integral transformation is difficult to perform, and inverse transformation is needed. This process inevitably produces truncation and discrete errors [31–33]. The governing equations can be directly solved in the time domain by using the finite element method, thereby avoiding the tedious processes in integral transformation. This method may be more efficient and may have higher precision. Furthermore, the time history of variables in constitutive relations can be reflected. Tian et al. [34] solved 2D generalized thermoelasticity problems by using a direct finite element method, which decreases the solving difficulty in the 2D model due to integral transformation. Li et al. [35] analyzed the nonlinear transient response under the generalized thermal diffusion theory based on the time-domain finite element method and obtained a good effect.

This paper investigates the transient thermal shock problem for fiber-reinforced materials with a time-dependent variable thermal conductivity according to the L-S theory. Time-domain finite element method is applied to derive the nonlinear governing equations. Numerical examples are presented to clarify the transient thermal shock response on a half-space. Field quantities are obtained for different thermal conductivities and illustrated graphically.

2. Governing Equations

Belfield et al. [5] proposed a constitutive equation for a fiber-reinforced linearly thermoelastic anisotropic medium in studying the deformation of fiber-reinforced composites. Given the reinforced direction $a \equiv (a_1, a_2, a_3)$, $a_1^2 + a_2^2 + a_3^2 = 1$, and with consideration of variable thermal conductivity, the constitutive equations can be expressed as

$$\begin{aligned}\sigma_{ij} = {} & \lambda e_{kk}\delta_{ij} + 2\mu_T e_{ij} + \alpha\left(a_k a_m e_{km}\delta_{ij} + a_i a_j e_{kk}\right) \\ & + 2\left(\mu_L - \mu_T\right)\left(a_i a_k e_{kj} + a_j a_k e_{ki}\right) \\ & + \beta a_k a_m e_{km} a_i a_j - \gamma\theta\delta_{ij},\end{aligned} \tag{1}$$

$$\rho S = \gamma e_{kk} + \frac{\rho C_E}{T_0}\theta, \tag{2}$$

where σ_{ij} is the stress tensor; δ_{ij} is the Kronecker delta; e_{ij} is the strain tensor; α, β, $(\mu_L - \mu_T)$, and γ are reinforcement parameters, with $\gamma = (3\lambda + 2\mu)\alpha_t$, in which λ and μ are Lame constants; α_t is the coefficient of linear thermal expansion; T_0 is the reference temperature; $\theta = T - T_0$, in which θ is the temperature difference; S is the entropy density; ρ is the mass density; C_E is the specific heat at constant strain; and $e_{kk} = u_{,x} + v_{,y}$.

The equation of motion (in the context of L-S theory) is

$$\sigma_{ij,j} = \rho\ddot{u}_i, \tag{3}$$

where u_i is the displacement vector.

The equation of energy conservation is

$$q_{i,i} = -\rho T_0 \dot{S}, \tag{4}$$

where q_i is the heat flux vector.

The geometrical equation is

$$e_{ij} = \frac{1}{2}\left(u_{i,j} + u_{j,i}\right). \tag{5}$$

The fiber-reinforced direction is defined as $a \equiv (1, 0, 0)$, $(\partial/\partial z) \equiv 0$, and $w = 0$. Thus, equation (1) can be written as

$$\begin{aligned}\sigma_{xx} &= A_{11}u_{,x} + A_{12}v_{,y} - \gamma\theta,\\ \sigma_{yy} &= A_{12}u_{,x} + A_{22}v_{,y} - \gamma\theta,\\ \sigma_{xy} &= \mu_L\left(u_{,y} + v_{,x}\right),\end{aligned} \tag{6}$$

$$\sigma_{xz} = \sigma_{yz} = 0, \tag{7}$$

where

$$\begin{aligned}A_{11} &= \lambda + 2\left(\alpha + \mu_T\right) + 4\left(\mu_L - \mu_T\right) + \beta,\\ A_{12} &= \lambda + \alpha,\\ A_{22} &= \lambda + 2\mu_T.\end{aligned} \tag{8}$$

From equations (5) and (7), equation (3) yields

$$\begin{aligned}\rho\frac{\partial^2 u}{\partial t^2} &= A_{11}\frac{\partial^2 u}{\partial x^2} + C_2\frac{\partial^2 v}{\partial x\partial y} + C_1\frac{\partial^2 u}{\partial y^2} - \gamma\frac{\partial\theta}{\partial x},\\ \rho\frac{\partial^2 v}{\partial t^2} &= A_{22}\frac{\partial^2 v}{\partial y^2} + C_2\frac{\partial^2 u}{\partial x\partial y} + C_1\frac{\partial^2 v}{\partial x^2} - \gamma\frac{\partial\theta}{\partial y},\end{aligned} \tag{9}$$

where

$$\begin{aligned}C_1 &= \mu_L,\\ C_2 &= \alpha + \lambda + \mu_L.\end{aligned} \tag{10}$$

The equation of heat conduction is

$$q_i + \tau_0\dot{q}_i = -K\theta_{,i}, \tag{11}$$

where τ_0 is the relaxation time.

The thermal conductivity K is temperature dependent and assumed to have the following linear form:

$$K = K(\theta) = K_0\left(1 + K_1\theta\right), \tag{12}$$

where K_0 is the initial thermal conductivity and K_1 is the small quantity for measuring the influence of temperature on thermal conductivity.

From equations (2) and (4), equation (11) then yields

$$\left(K\theta_{,i}\right)_{,i} = \frac{\partial}{\partial t}\left(1 + \tau_0\frac{\partial}{\partial t}\right)\left(\rho C_E\theta + T_0\gamma e_{kk}\right). \tag{13}$$

3. Finite Element Formulations

The finite element method is an approximate method for solving differential equations. The first step in solving the problem is to establish the governing equations, followed by defining the boundary conditions based on the specific problems and then performing the the structural discrete, unit analysis and overall analysis to obtain the numerical solutions. For nonlinear problems, the finite element expression is obtained using the finite element method, which can eliminate the influence of truncation errors and avoid the tediousness of integral transformation. In addition, the time history of the variables in the constitutive relation can be determined to better reflect the wavefront characteristics. FlexPDE is a useful tool for solving partial differential equations, which can form Galerkin finite element integrals, derivatives, and dependencies aiming at the problem description and then build a coupling matrix and solve it. Therefore, FlexPDE is employed to deal with the related partial differential equations generated by the finite element method. For convenience, the constitutive equations of equations (1) and (2) can be expressed in the matrix form as follows:

$$\begin{aligned}\{\sigma\} &= \left[C_e\right]\{e\} - \{\gamma\}\theta,\\ \rho S &= \{\gamma\}^{\mathrm{T}}\{e\} + \frac{\rho C_E}{T_0}\theta.\end{aligned} \tag{14}$$

The heat conduction equation of equation (11) can be written as

$$\{q\} + \tau_0\{\dot{q}\} = -[K]\{\theta'\}. \tag{15}$$

The basic variables in this study include displacement and temperature. After the elements are divided, the variables are represented by shape functions in each element as follows:

$$\begin{aligned}\{u\} &= \left[N_1^e\right]\{u^e\},\\ \{\theta\} &= \left[N_2^e\right]^{\mathrm{T}}\{\theta^e\},\end{aligned} \tag{16}$$

where $\{u^e\}$ and $\{\theta^e\}$ are the nodal displacement and temperature, respectively. $[N_1^e]$ and $[N_2^e]^{\mathrm{T}}$ are shape functions:

$$\begin{aligned}\left[N_1^e\right] &= \begin{bmatrix} N_1 & 0 & N_2 & 0 & \ldots & N_n & 0\\ 0 & N_1 & 0 & N_2 & \ldots & 0 & N_n\end{bmatrix},\\ \left[N_2^e\right]^T &= \left[N_1 \;\; N_2 \;\; \ldots \;\; N_n\right],\end{aligned} \tag{17}$$

where n denotes the number of nodes in the grid.

According to equation (5) and given $\theta' = \theta_{,i}$, equation (15) yields

$$\begin{aligned}\{e\} &= \left[B_1\right]\{u^e\},\\ \{\theta'\} &= \left[B_2\right]\{\theta^e\},\end{aligned} \tag{18}$$

where $[B_1]$ and $[B_2]$ are the first-order derivative of the components in $[N_1^e]$ and $[N_2^e]$ with respect to the material coordinates, respectively.

Then, the variational forms of equation (5) are

$$\begin{aligned}\delta\{e\} &= \left[B_1\right]\delta\{u^e\},\\ \delta\{\theta'\} &= \left[B_2\right]\delta\{\theta^e\}.\end{aligned} \tag{19}$$

According to virtual displacement principles, the fiber-reinforced generalized thermoelasticity problem with variable thermal conductivity can be formulated as

$$\begin{aligned}&\int_V\left[\delta\{e\}^{\mathrm{T}}\{\sigma\} + \delta\{\theta'\}^{\mathrm{T}}\left(\{q\} + \tau_0\{\dot{q}\}\right) - \rho T_0\delta\{\theta\}^{\mathrm{T}}\left(\{\dot{S}\} + \tau_0\{\ddot{S}\}\right)\right]\\ &dV = -\int_V\delta\{u\}^{\mathrm{T}}\rho\{\ddot{u}\}dV + \int_{A_\sigma}\delta\{u\}^{\mathrm{T}}\{\overline{F}\}dA + \int_{A_q}\delta\{\theta\}^{\mathrm{T}}\overline{q}\,dA,\end{aligned} \tag{20}$$

where $\{\overline{F}\}$ is the traction vector.

According to equations (13)–(15), and (19), equation (20) yields

$$\int_V \delta\{e\}^{\mathrm{T}}\{\sigma\}dV = \delta\{u^e\}^{\mathrm{T}}\left([K^e_{mm}]\{u^e\} - [K^e_{m\theta}]\{\theta^e\}\right),$$
$$\int_V \delta\{\theta'\}^{\mathrm{T}}\left(\{q\} + \tau_0\{\dot{q}\}\right)dV = -\delta\{\theta^e\}^{\mathrm{T}}[K^e_{\theta\theta}]\{\theta^e\},$$
$$-\int_V \rho T_0 \delta\{\theta\}^{\mathrm{T}}\Big(\{\dot{S}\} + \tau_0\{\ddot{S}\}\Big)dV = -\delta\{\theta^e\}^{\mathrm{T}}\Big([C^e_{\theta m}]\{\dot{u}^e\} + [C^e_{\theta\theta}]\{\dot{\theta}\} + [M^e_{\theta m}]\{\ddot{u}^e\} + [M^e_{\theta\theta}]\{\ddot{\theta}\}\Big),$$
$$-\int_V \delta\{u\}^{\mathrm{T}}\rho\{\ddot{u}\}dV = -\delta\{u^e\}^{\mathrm{T}}[M^e_{mm}]\{\ddot{u}^e\},$$
$$\int_{A_\sigma} \delta\{u\}^{\mathrm{T}}\{\overline{F}\}dA = \delta\{u^e\}^{\mathrm{T}}[F^e_m],$$
$$\int_{A_q} \delta\{\theta\}^{\mathrm{T}}\theta\overline{q}\,dA = \delta\{\theta^e\}^{\mathrm{T}}\{T^e_\theta\}. \tag{21}$$

These expressions can be summed as the following matrix form:

$$\begin{bmatrix} M^e_{mm} & 0 \\ M^e_{\theta m} & M^e_{\theta\theta} \end{bmatrix}\begin{Bmatrix} \ddot{u}^e \\ \ddot{\theta}^e \end{Bmatrix} + \begin{bmatrix} 0 & 0 \\ C^e_{\theta m} & C^e_{\theta\theta} \end{bmatrix}\begin{Bmatrix} \dot{u}^e \\ \dot{\theta}^e \end{Bmatrix} + \begin{bmatrix} K^e_{mm} & -K^e_{m\theta} \\ 0 & K^e_{\theta\theta} \end{bmatrix}\begin{Bmatrix} u^e \\ \theta^e \end{Bmatrix} = \begin{Bmatrix} F^e_m \\ -T^e_\theta \end{Bmatrix}, \tag{22}$$

where

$$[K^e_{mm}] = \int_V [B_1]^{\mathrm{T}}\{C_e\}[B_1]dV,$$
$$[K^e_{m\theta}] = \int_V [B_1]^{\mathrm{T}}\{\gamma\}[N^e_2]^{\mathrm{T}}dV,$$
$$[K^e_{\theta\theta}] = \int_V [B_2]^{\mathrm{T}}[K][B_2]dV,$$
$$[C^e_{\theta m}] = \int_V T_0[N^e_2]\{\gamma\}^{\mathrm{T}}[B_1]dV,$$
$$[C^e_{\theta\theta}] = \int_V T_0[N^e_2]\frac{\rho C_E}{T_0}[N^e_2]^{\mathrm{T}}dV,$$
$$[M^e_{\theta m}] = \int_V T_0[N^e_2]\tau_0\{\gamma\}^{\mathrm{T}}[B_1]dV, \tag{23}$$
$$[M^e_{\theta\theta}] = \int_V T_0[N^e_2]\tau_0\frac{\rho C_E}{T_0}[N^e_2]^{\mathrm{T}}dV,$$
$$[M^e_{mm}] = \int_V [N^e_1]^{\mathrm{T}}\rho[N^e_1]dV,$$
$$[F^e_m] = \int_{A_\sigma} [N^e_1]^{\mathrm{T}}\{\overline{F}\}dA,$$
$$\{T^e_\theta\} = \int_{A_q} [N^e_2]\overline{q}\,dA.$$

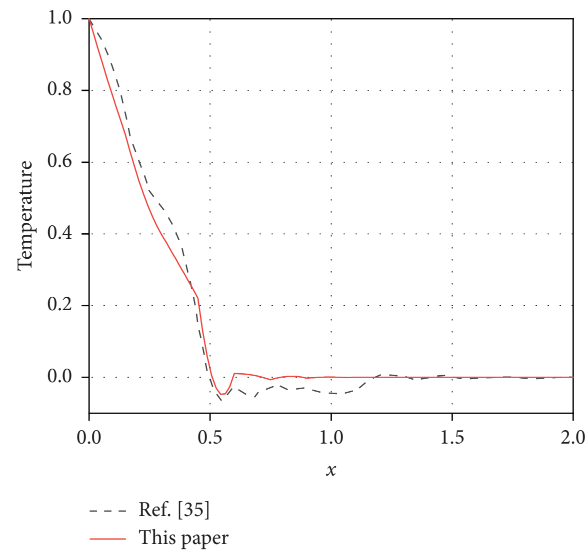

Figure 1: Distribution of temperature along the x-axis at $t = 0.06$.

4. Numerical Results and Discussion

4.1. Verification. To check the validity of the proposed method, reference [35] is chosen for comparison. Li et al. [35] had investigated the generalized diffusion-thermo-elasticity problems with variable thermal conductivity by using the finite element method and had verified its effectiveness. This comparison research is conducted without the consideration of diffusion. In addition to this, the numerical model, initial conditions, and boundary conditions are same with reference [35]. The distribution of the temperature profile at the dimensionless time $t = 0.06$ is shown graphically in Figure 1, from which a trend consistency can be observed. This guarantees the validity and accuracy of the present method.

4.2. Results and Discussion. Consider the problem of a fiber-reinforced anisotropic elastic half-space ($x \geq 0$) with variable thermal conductivity. As shown in Figure 2(a), the boundary surface is assumed to be without traction, and the banded area on $x = 0$ is subjected to a time-dependent transient thermal shock.

Initial conditions:

$$u(x, y, 0) = v(x, y, 0) = \theta(x, y, 0) = 0,$$
$$\frac{\partial u(x, y, 0)}{\partial t} = \frac{\partial v(x, y, 0)}{\partial t} = \frac{\partial \theta(x, y, 0)}{\partial t} = 0. \tag{24}$$

Boundary conditions:

$$\sigma_{xx}(0, y, t) = \sigma_{xy}(0, y, t) = 0, \tag{25}$$

$$\theta(0, y, t) = H(t)H(L - |y|), \tag{26}$$

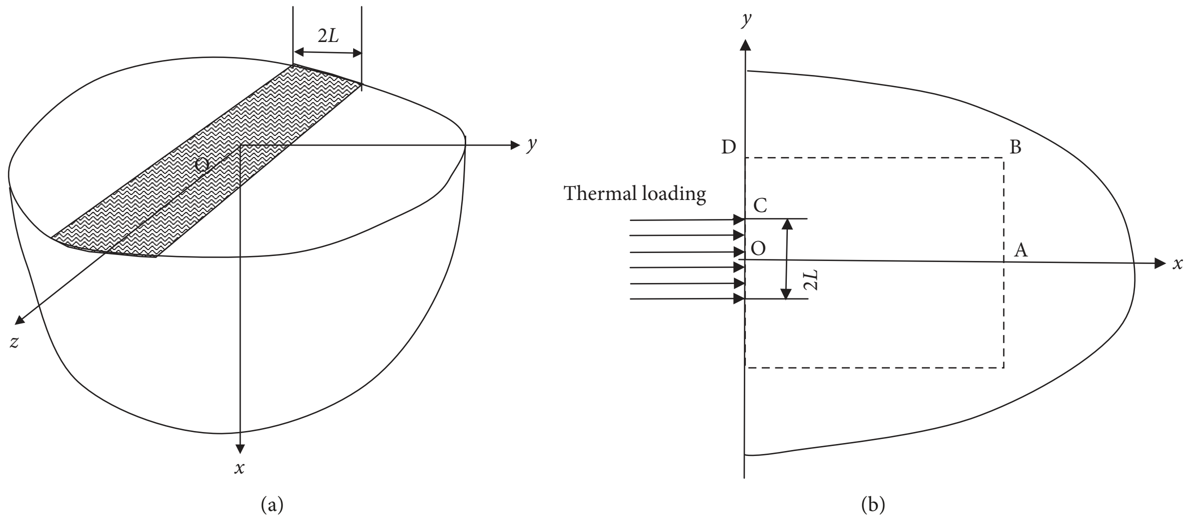

FIGURE 2: (a) Diagram of a half-space under thermal shock. (b) Simplified xy plane diagram of the half-space.

where $H(\cdot)$ is the Heaviside unit step function.

Under the given conditions, the half-space model can be simplified as a xy plane model, as shown in Figure 2(b). The components of displacement and temperature can be simplified as follows:

$$\begin{aligned} u_x &= u(x, y, t), \\ u_y &= v(x, y, t), \\ u_z &= 0, \\ \theta &= \theta(x, y, t). \end{aligned} \tag{27}$$

Copper material is selected for numerical evaluation, and the parameters are presented in Table 1 [36].

For convenience, the following nondimensional quantities are introduced:

$$\begin{aligned} (x^*, y^*, u^*, v^*) &= c_1\eta(x, y, u, v), \\ t^* &= c_1^2\eta t, \\ \tau_0^* &= c_1^2\eta\tau_0, \\ \theta^* &= \frac{\gamma}{\lambda + 2\mu_T}\theta, \\ K_1^* &= \frac{\lambda + 2\mu_T}{\gamma}K_1, \quad i, j = 1, 2, \\ {\sigma_{ij}}^* &= \frac{\sigma_{ij}}{\lambda + 2\mu_T}, \\ \eta &= \frac{\rho C_E}{K_0}, \\ c_1^2 &= \frac{\lambda + 2\mu_T}{\rho}. \end{aligned} \tag{28}$$

According to equation (28), equations (7), (9), and (12) can be written as follows (the asterisk is removed for brevity):

$$\begin{aligned} \sigma_{xx} &= h_{11}\frac{\partial u}{\partial x} + h_{12}\frac{\partial v}{\partial y} - \theta, \\ \sigma_{yy} &= h_{22}\frac{\partial v}{\partial y} + h_{12}\frac{\partial u}{\partial x} - \theta, \\ \sigma_{xy} &= \frac{\mu_L}{\lambda + 2\mu_T}\left(\frac{\partial u}{\partial y} + \frac{\partial v}{\partial x}\right), \end{aligned} \tag{29}$$

$$\begin{aligned} \frac{\partial^2 u}{\partial t^2} &= h_{11}\frac{\partial^2 u}{\partial x^2} + h_2\frac{\partial^2 v}{\partial x\partial y} + h_1\frac{\partial^2 u}{\partial y^2} - \frac{\partial\theta}{\partial x}, \\ \frac{\partial^2 v}{\partial t^2} &= h_{22}\frac{\partial^2 v}{\partial y^2} + h_2\frac{\partial^2 u}{\partial x\partial y} + h_1\frac{\partial^2 v}{\partial x^2} - \frac{\partial\theta}{\partial y}, \end{aligned} \tag{30}$$

$$\begin{aligned} \frac{\partial}{\partial t}\left(1 + \tau_0\frac{\partial}{\partial t}\right)\left[\varepsilon\left(\frac{\partial u}{\partial x} + \frac{\partial v}{\partial y}\right) + \theta\right] = (1 + K_1\theta)\left(\frac{\partial^2\theta}{\partial x^2} + \frac{\partial^2\theta}{\partial y^2}\right) \\ + K_1\left[\left(\frac{\partial\theta}{\partial x}\right)^2 + \left(\frac{\partial\theta}{\partial y}\right)^2\right], \end{aligned} \tag{31}$$

where

$$\begin{aligned} (h_{11}, h_{22}, h_{12}, h_1, h_2) &= \frac{(A_{11}, A_{22}, A_{12}, C_1, C_2)}{\lambda + 2\mu_T}, \\ \varepsilon &= \frac{\gamma^2 T_0}{\rho C_E(\lambda + 2\mu_T)}, \end{aligned} \tag{32}$$

Under the given conditions of equations (24)–(27), the nonlinear governing equations (29)–(31) can be solved directly in the time domain. Under the given conditions, the research model is symmetrical about the x-axis. Thus, the

Table 1: Material parameters of the copper material.

$\lambda = 7.76 \times 10^{10}\ \mathrm{N/m^2}$	$\alpha_t = 1.78 \times 10^{-5} \cdot \mathrm{K^{-1}}$	$\eta = 8886.73\ \mathrm{s/m^2}$	$C_E = 383.1\ \mathrm{J/(kg\,K)}$
$\rho = 8954\ \mathrm{kg/m^3}$	$K_0 = 386\ \mathrm{W/(m\,K)}$	$T_0 = 293\ \mathrm{K}$	$\alpha = -1.28 \times 10^{10}\ \mathrm{N/m^2}$
$\beta = 0.32 \times 10^{10}\ \mathrm{N/m^2}$	$\mu_L = 2.45 \times 10^{10}\ \mathrm{N/m^2}$	$\mu_T = 1.89 \times 10^{10}\ \mathrm{N/m^2}$	

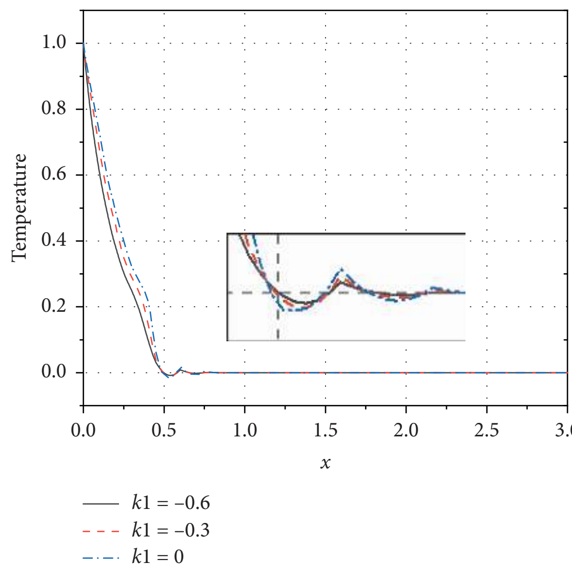

Figure 3: Distribution of nondimensional temperature along OA.

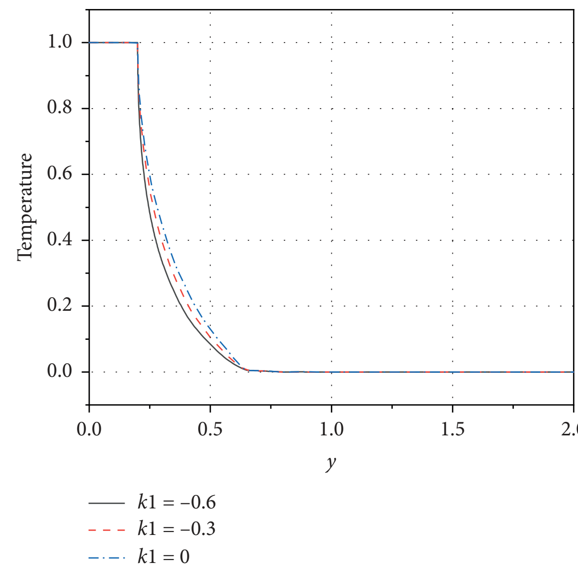

Figure 4: Distribution of nondimensional temperature along OD.

rectangular area OABD is used for the subsequent analysis for simplification.

The dimensionless distributions of temperature, displacement, and stress are illustrated graphically in Figures 3–8. The K_1 value is expressed in four cases to discuss the effects of variable thermal conductivity as follows:

(1) Case 1: $K_1 = -0.6$

(2) Case 2: $K_1 = -0.3$

(3) Case 3: $K_1 = 0$.

Figures 3 and 4 show the distributions of nondimensional temperature along OA and OD. The dimensionless temperature is equal to 1 at $x = 0$ and $0 \leq y \leq 0.2$ region, which agrees with the boundary conditions that were previously assigned. As the thermal conductivity increases, the temperatures along OA and OD increase. This result indicates that the coefficient of thermal conductivity is positively correlated with the temperature change, and that variable thermal conductivity significantly affects the temperature distribution. Moreover, the wavefront effect is more pronounced as the thermal conductivity increases. There is a diverse trend at $x = 0.5$ in Figure 3, which is mainly caused by the effect of wavefront and the calculation errors.

Given that the research model is symmetrical about the x-axis, the vertical displacement along $u_{y-\mathrm{OA}}$ is zero and need not be considered. Figure 5 depicts the distribution of the nondimensional horizontal displacement $u_{x-\mathrm{OA}}$, which shows that the closest section to the origin undergoes expansion, the next undergoes compression, and the rest away

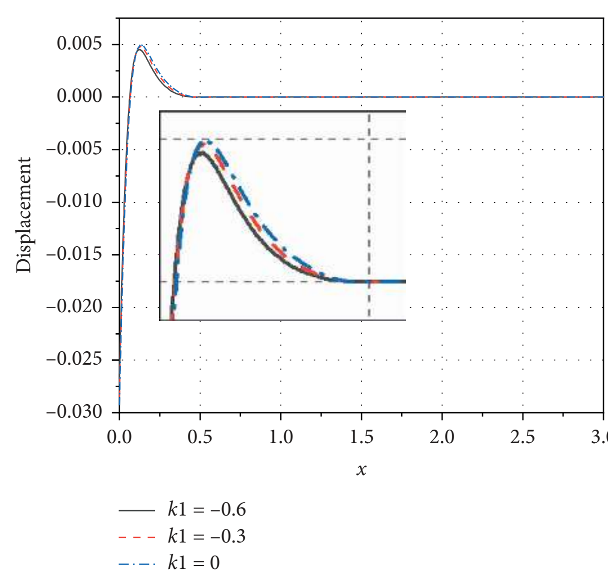

Figure 5: Distribution of nondimensional horizontal displacement along OA.

from the origin is undisturbed. Figure 5 demonstrates that variable thermal conductivity is positively correlated with the distribution of the horizontal displacement along OA.

Figures 6 and 7 show the distribution of the nondimensional horizontal displacement $u_{x-\mathrm{OD}}$ and the vertical displacement $u_{y-\mathrm{OD}}$, respectively. As shown, the variable thermal conductivity obviously affected the distribution of displacement. In addition, $y = 0.2$ is the most affected

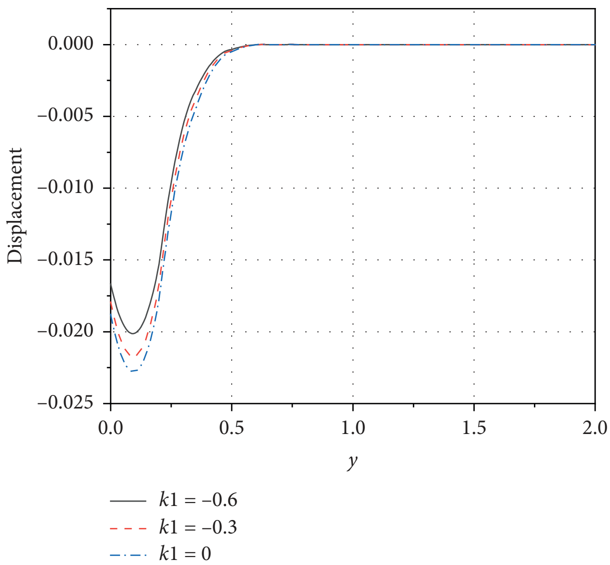

FIGURE 6: Distribution of the nondimensional horizontal displacement along OD.

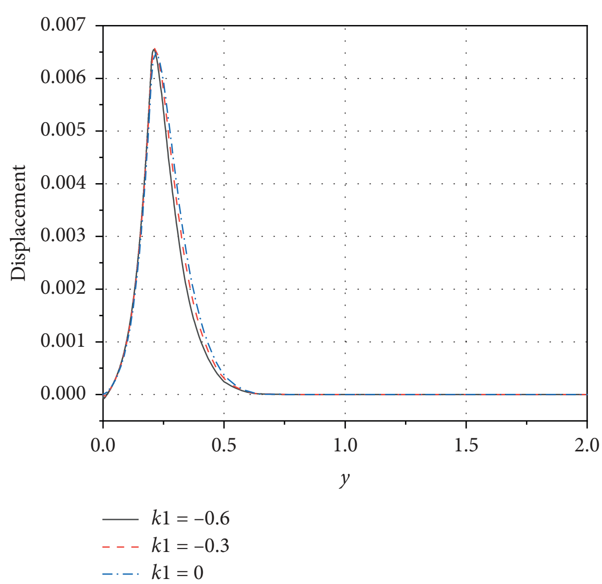

FIGURE 7: Distribution of the nondimensional vertical displacement along OD.

thermal shock boundary point. The negative value in Figure 6 indicates that the particles tend to move toward the unconstrained direction.

Figure 8 shows the distribution of the nondimensional stress $\sigma_{yy-\mathrm{OD}}$. The stress values show a violent oscillation in the $0 < y < 0.2$ zone, and variable thermal conductivity obviously affects the distribution of stress along OD, particularly in the $0.2 < y < 0.8$ zone.

5. Concluding Remarks

It is well known that instantaneous changes of temperature can markedly change the thermal conductivity of a material.

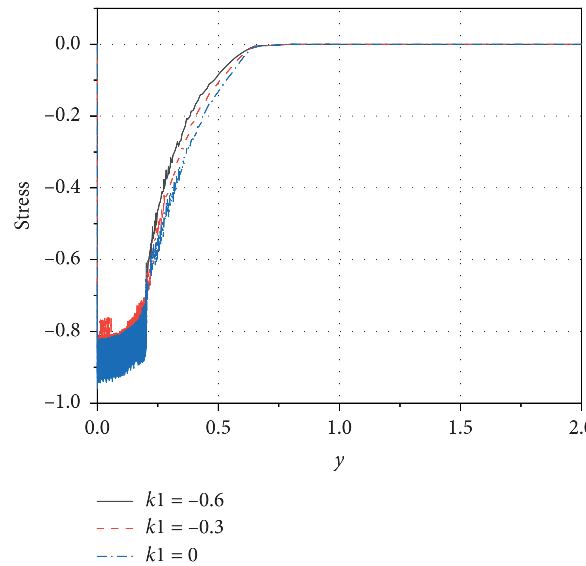

FIGURE 8: Distribution of the nondimensional stress σ_{yy} along OD.

Therefore, this article investigated the effect of temperature-dependent variable thermal conductivity on a fiber-reinforced generalized thermoelastic half-space. Given the reinforced direction $a = (1, 0, 0)$, a region of its surface is subjected to a transient thermal shock. The problem is studied in the context of L-S theory. The time-domain finite element method is proposed to analyze the nonlinear response.

Based on the simulation, we can draw that the time-finite element method is very effective for analyzing nonlinear problems with given initial and boundary conditions, and by which we can capture a pronounced wavefront effect. In consideration of the fiber-reinforced effect, variable thermal conductivity positively affects the distributions of temperature, displacement, and stress. In addition, the boundary point of thermal shock is affected the most.

Nomenclature

σ_{ij}:	Components of stress tensor
δ_{ij}:	Kronecker delta
e_{ij}:	Components of strain tensor
α, β, and $\mu_L - \mu_T$:	Reinforcement parameters
λ, μ:	Lame constants
α_t:	Coefficient of linear thermal expansion
γ:	$(3\lambda + 2\mu)\alpha_t$
T_0:	Reference temperature
θ:	Temperature difference
S:	Entropy density
ρ:	Mass density
C_E:	Specific heat at constant strain
u_i:	Displacement vector
e_{kk}:	$u_{,x} + v_{,y}$
q_i:	Heat flux vector
τ_0:	Relaxation time
K_0:	Initial thermal conductivity

K_1: Small quantity for measuring the influence of temperature on thermal conductivity
n: Number of nodes in the grid
$H(\cdot)$: Heaviside unit step function
$[N_1^e]$ and $[N_2^e]^{\mathrm{T}}$: Shape functions
$[B_1]$ and $[B_2]$: First-order derivative of $[N_1^e]$ and $[N_2^e]$ with respect to the material coordinates
$\{\overline{F}\}$: Traction vector.

Data Availability

All the data used to support the findings of this study are included within the article.

Conflicts of Interest

There are no conflicts of interest regarding the publication of this paper.

References

[1] A. J. M. Spencer, *Deformations of Fibre–Reinforced Materials*, Oxford University Press, New York, NY, USA, 1972.

[2] M. I. A. Othman and I. A. Abbas, "Effect of rotation on plane waves at the free surface of a fibre-reinforced thermoelastic half-space using the finite element method," *Meccanica*, vol. 46, no. 2, pp. 413–421, 2011.

[3] M. I. A. Othman and S. M. Said, "The effect of rotation on two-dimensional problem of a fiber-reinforced thermoelastic with one relaxation time," *International Journal of Thermophysics*, vol. 33, no. 1, pp. 160–171, 2012.

[4] M. I. A. Othman and S. M. Said, "The effect of mechanical force on generalized thermoelasticity in a fiber-reinforcement under three theories," *International Journal of Thermophysics*, vol. 33, no. 6, pp. 1082–1099, 2012.

[5] A. J. Belfield, T. G. Rogers, and A. J. M. Spencer, "Stress in elastic plates reinforced by fibres lying in concentric circles," *Journal of the Mechanics and Physics of Solids*, vol. 31, no. 1, pp. 25–54, 1983.

[6] S. M. Said and M. I. A. Othman, "Effect of mechanical force, rotation and moving internal heat source on a two-temperature fiber-reinforced thermoelastic medium with two theories," *Mechanics of Time-Dependent Materials*, vol. 21, no. 2, pp. 245–261, 2017.

[7] P. Lopato, G. Psuj, and B. Szymanik, "Nondestructive inspection of thin basalt fiber reinforced composites using combined terahertz imaging and infrared thermography," *Advances in Materials Science and Engineering*, vol. 2016, Article ID 1249625, 13 pages, 2016.

[8] K. Patel, R. Gupta, M. Garg, B. Wang, and U. Dave, "Development of FRC materials with recycled glass fibers recovered from industrial GFRP-acrylic waste," *Advances in Materials Science and Engineering*, vol. 2019, Article ID 4149708, 15 pages, 2019.

[9] M. A. Biot, "Thermoelasticity and irreversible thermodynamics," *Journal of Applied Physics*, vol. 27, no. 3, pp. 240–253, 1956.

[10] H. W. Lord and Y. Shulman, "A generalized dynamical theory of thermoelasticity," *Journal of the Mechanics and Physics of Solids*, vol. 15, no. 5, pp. 299–309, 1967.

[11] A. E. Green and K. A. Lindsay, "Thermoelasticity," *Journal of Elasticity*, vol. 2, no. 1, pp. 1–7, 1972.

[12] A. E. Green and P. M. Naghdi, "Thermoelasticity without energy dissipation," *Journal of Elasticity*, vol. 31, no. 3, pp. 189–208, 1993.

[13] M. I. A. Othman and K. Lotfy, "The effect of magnetic field and rotation of the 2-D problem of a fiber-reinforced thermoelastic under three theories with influence of gravity," *Mechanics of Materials*, vol. 60, no. 7, pp. 129–143, 2013.

[14] A. E. Abouelregal and A. M. Zenkour, "The effect of fractional thermoelasticity on a two-dimensional problem of a mode I crack in a rotating fiber-reinforced thermoelastic medium," *Chinese Physics B*, vol. 22, no. 10, article 108102, 8 pages, 2013.

[15] I. A. Abbas, "Analytical solutions of 2-D problem for cracked thermoelastic fiber-reinforced anisotropic material," *Theoretical and Applied Fracture Mechanics*, vol. 91, pp. 31–36, 2017.

[16] S. Singh, D. Kumar, and K. N. Rai, "Convective-radiative fin with temperature dependent thermal conductivity, heat transfer coefficient and wavelength dependent surface emissivity," *Propulsion and Power Research*, vol. 3, no. 4, pp. 207–221, 2014.

[17] A. S. V. Ravikanth and U. K. Niyan, "A haar wavelet study on convective-radiative fin under continuous motion with temperature-dependent thermal conductivity," *Walailak Journal of Science & Technology*, vol. 11, no. 3, pp. 211–224, 2014.

[18] A. S. Dogonchi and D. D. Ganji, "Convection–radiation heat transfer study of moving fin with temperature-dependent thermal conductivity, heat transfer coefficient and heat generation," *Applied Thermal Engineering*, vol. 103, pp. 705–712, 2016.

[19] T.-H. Park, N.-W. Park, J. Kim, W.-Y. Lee, J.-H. Koh, and S.-K. Lee, "Cross-plane temperature-dependent thermal conductivity of Al-doped zinc oxide thin films," *Journal of Alloys and Compounds*, vol. 638, pp. 83–87, 2015.

[20] W. Pan, F. Yi, Y. Zhu, and S. Meng, "Identification of temperature-dependent thermal conductivity and experimental verification," *Measurement Science & Technology*, vol. 27, no. 7, article 075005, 2016.

[21] M. I. A. Othman, R. S. Tantawi, and E. E. M. Eraki, "Effect of initial stress on a semiconductor material with temperature dependent properties under DPL model," *Microsystem Technologies*, vol. 23, no. 12, pp. 5587–5598, 2017.

[22] A. M. Zenkour and A. E. Abouelregal, "Nonlocal thermoelastic nanobeam subjected to a sinusoidal pulse heating and temperature-dependent physical properties," *Microsystem Technologies*, vol. 21, no. 8, pp. 1767–1776, 2015.

[23] C. Xiong and Y. Guo, "Effect of variable properties and moving heat source on magnetothermoelastic problem under fractional order thermoelasticity," *Advances in Materials Science and Engineering*, vol. 2016, Article ID 5341569, 12 pages, 2016.

[24] Y. Wang, D. Liu, Q. Wang, and J. Zhou, "Asymptotic solutions for generalized thermoelasticity with variable thermal material properties," *Archives of Mechanics*, vol. 68, no. 3, pp. 181–202, 2016.

[25] M. A. Ezzat and A. A. El-Bary, "On thermo-viscoelastic infinitely long hollow cylinder with variable thermal conductivity," *Microsystem Technologies*, vol. 23, no. 8, pp. 3263–3270, 2017.

[26] S. M. Abo-Dahab and I. A. Abbas, "LS model on thermal shock problem of generalized magneto-thermoelasticity for an infinitely long annular cylinder with variable thermal

conductivity," *Applied Mathematical Modelling*, vol. 35, no. 8, pp. 3759–3768, 2011.

[27] C. Li, H. Guo, X. Tian, and X. Tian, "Transient response for a half-space with variable thermal conductivity and diffusivity under thermal and chemical shock," *Journal of Thermal Stresses*, vol. 40, no. 3, pp. 389–401, 2016.

[28] T. He and Y. Guo, "A one-dimensional thermoelastic problem due to a moving heat source under fractional order theory of thermoelasticity," *Advances in Materials Science and Engineering*, vol. 2014, Article ID 510205, 9 pages, 2014.

[29] A. M. Abd El-Latief, "Application of generalized fractional thermoelasticity theory with two relaxation times to an electromagnetothermoelastic thick plate," *Advances in Materials Science and Engineering*, vol. 2016, Article ID 5821604, 9 pages, 2016.

[30] C. Li, H. Guo, and X. Tian, "Transient responses of generalized magnetothermoelasto-diffusive problems with rotation using Laplace transform–finite element method," *Journal of Thermal Stresses*, vol. 40, no. 9, pp. 1–14, 2017.

[31] M. A. Ezzat and A. A. El-Bary, "Effects of variable thermal conductivity and fractional order of heat transfer on a perfect conducting infinitely long hollow cylinder," *International Journal of Thermal Sciences*, vol. 108, pp. 62–69, 2016.

[32] H. Sherief and A. M. Abd El-Latief, "Effect of variable thermal conductivity on a half-space under the fractional order theory of thermoelasticity," *International Journal of Mechanical Sciences*, vol. 74, pp. 185–189, 2013.

[33] H. H. Sherief and F. A. Hamza, "Modeling of variable thermal conductivity in a generalized thermoelastic infinitely long hollow cylinder," *Meccanica*, vol. 51, no. 3, pp. 551–558, 2016.

[34] X. Tian, Y. Shen, C. Chen, and T. He, "A direct finite element method study of generalized thermoelastic problems," *International Journal of Solids and Structures*, vol. 43, no. 7-8, pp. 2050–2063, 2006.

[35] C. Li, H. Guo, and X. Tian, "Time-domain finite element analysis to nonlinear transient responses of generalized diffusion-thermoelasticity with variable thermal conductivity and diffusivity," *International Journal of Mechanical Sciences*, vol. 131-132, pp. 234–244, 2017.

[36] H. H. Sherief and K. A. Helmy, "A two-dimensional problem for a half-space in magneto-thermoelasticity with thermal relaxation," *International Journal of Engineering Science*, vol. 40, no. 5, pp. 587–604, 2002.